Chapter 11
Experimental Study of Flow Structure and Turbulent Characteristics in Lead–Bismuth Two-Phase Flow

Gen Ariyoshi, Daisuke Ito, and Yasushi Saito

Abstract In a severe accident of a lead–bismuth-cooled accelerator-driven system, a gas–liquid two-phase flow with a large liquid-to-gas density ratio might appear, such as a steam leakage into hot lead–bismuth flow. It is still difficult to predict such phenomena because there are no available flow models for two-phase flow with a large density ratio compared to ordinary two-phase flows such as an air–water two-phase flow. Therefore, a two-phase flow model should be developed based on experimental data of two-phase flows with a large density ratio. In this study, a liquid–metal two-phase flow was measured by using a four-sensor electrical conductivity probe and a miniature electromagnetic probe to establish an experimental database for lead–bismuth flow structure. In measurements with the four-sensor probe, the radial profiles of void fraction and interfacial area concentration were measured at different axial positions. Experiments were also performed to understand the turbulent structure in a liquid–metal two-phase flow by using the electromagnetic probe. From the data measured by both four-sensor and electromagnetic probes, it is shown that the turbulence intensity at the pipe center was proportional to the void fraction to the power of 0.8 for higher void fraction. These results represented a similar tendency as previous data in air–water two-phase flows.

Keywords Accelerator-driven system • Electromagnetic probe • Four-sensor probe • Lead–bismuth • Turbulence characteristics • Two-phase flow • Void fraction

G. Ariyoshi (✉)
Graduate School of Energy Science, Kyoto University, Kyoto, Japan
e-mail: ariyoshi.gen.46n@st.kyoto-u.ac.jp

D. Ito • Y. Saito
Kyoto University Research Reactor Institute, Osaka, Japan

K. Nakajima (ed.), *Nuclear Back-end and Transmutation Technology for Waste Disposal*, DOI 10.1007/978-4-431-55111-9_11

11.1 Introduction

The accelerator-driven system (ADS) has been developed as the next-generation nuclear energy system and is expected to be used as a nuclear transmutation process [1]. ADS is a hybrid system that consists of a high-intensity proton accelerator, a nuclear spallation target, and a subcritical core. Lead–bismuth eutectic (LBE) is considered as an option of the spallation target and can also be used as the coolant of the reactor. Neutrons are produced by a nuclear spallation reaction between the protons supplied from the accelerator and the LBE target, and a chain reaction of nuclear fission can then be maintained by the contribution of spallation neutrons. The chain reaction in the core will stop when the supply of protons stops. Therefore, the ADS has a higher safety margin, in principle, than other nuclear energy systems.

As research toward the development of the ADS, a subcritical reactor physics study, a reactor thermal-hydraulics study, and studies on the material, accelerator, and fuel for the ADS have been carried out. However, safety assessment is very important in preparation for a possible severe accident. A pipe rupture in a steam generator is one of the severe accidents of a LBE-cooled ADS. In this case, the direct contact between the LBE and the water ejected from the ruptured pipe of the steam generator might lead to LBE–steam two-phase flow in the reactor pool. If the gas bubble comes into the fuel region, the core reactivity might be affected. Thus, the gas–liquid two-phase flow appearing in the ADS core should be understood in taking measures for such an accident. The gas–liquid two-phase flow in an ADS has density ratio that is an order larger than that of air–water two-phase flow. Although flow models of gas–liquid two-phase flow with a large liquid-to-gas density ratio are required for severe accident analysis, there are fewer studies on two-phase flow in the physical property range of large density ratio mixture. Thus, an experimental database on two-phase flow properties in two-phase flow with a large density ratio should be built and the two-phase flow model should be developed based on the database. In this study, an LBE two-phase flow was measured by using a four-sensor electrical conductivity probe and a miniature electromagnetic probe, and knowledge of the flow structure and the turbulent characteristics in two-phase flow with a large density ratio was obtained.

11.2 Measurement Techniques

11.2.1 Four-Sensor Probe

The four-sensor probe [2] used in this study consists of a central front sensor and three peripheral rear sensors (Fig. 11.1a). Tungsten acupuncture needles with a maximum diameter of 0.1 mm were coated with epoxy resin varnish except the tip; the diameter of the tip is less than 1 μm. The insulated needles were inserted into a

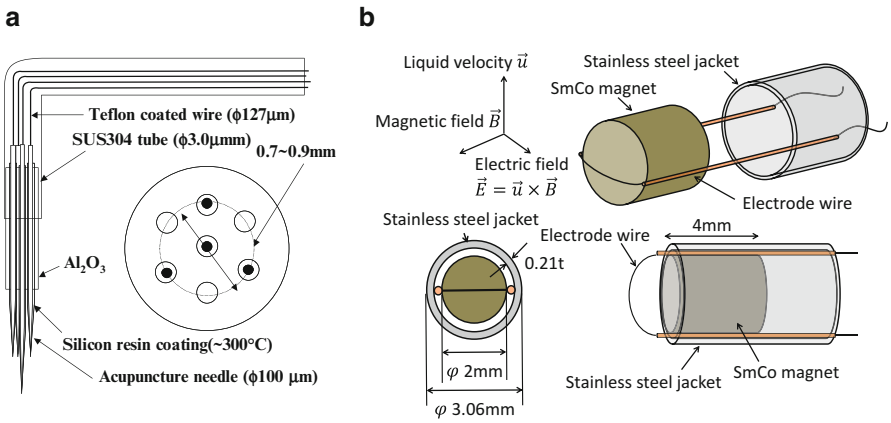

Fig. 11.1 Schematics of four-sensor probe (**a**) and electromagnetic probe (**b**)

seven-bore insulating tube made of Al_2O_3. The output signals were acquired at a sampling frequency of 10 kHz and then processed on a PC.

11.2.2 Electromagnetic Probe

The schematic of the electromagnetic probe [3, 4] used in this study is shown in Fig. 11.1b. The probe consists of a SmCo magnet, electrode wires, and a stainless steel jacket. Because a small cylindrical magnet with a diameter of 2 mm was used to miniaturize probe size, the induced potential between the electrodes at the tip of the probe was rather small. Therefore, the detected signal was amplified by a low-noise pre-amplifier and a DC amplifier. The signals digitized by an A/D converter were processed on a PC. The sampling frequency was 10 kHz.

The principle of the electromagnetic probe is based on Faraday's law. When the conducting fluid passes across a magnetic field, potential is induced in a direction normal to the magnetic field and the fluid velocity. Here, the induced potential is proportional to the velocity. In this study, the calibration of the electromagnetic probe was carried out using a rigid rotating setup (Fig. 11.2a) that consists of a cylindrical tank, a rotating system, and a heater. The tank was filled with LBE and rotated at a constant speed. The probe was inserted into the molten LBE rotating rigidly in the tank. The voltage corresponding to the tangential velocity component was measured, and this calibration was performed for all probes used in this study. Typical calibration results are shown in Fig. 11.2b.

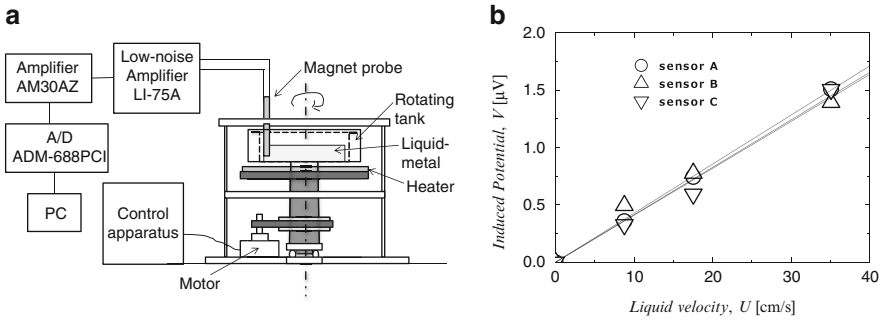

Fig. 11.2 Schematic of calibration system (**a**) and typical calibration results (**b**)

11.3 Experimental Setup

The schematic diagram of the LBE test loop is illustrated in Fig. 11.3. The test loop consists of a test section, a gas injector, an electromagnetic pump, a flow meter, and a drain tank. The test section is a stainless steel pipe with an inner diameter of 50 mm and a length of 2,000 mm. The working fluids are molten LBE and nitrogen gas. The flow rate of LBE was measured by the magnetic flow meter. Nitrogen gas was injected into LBE flow by the gas injector, which consists of 101 stainless steel needle tubes 0.58 mm in inner diameter. The gas flow rate was controlled by a mass flow controller. The operating temperature of this loop was maintained at 200 °C and the heating power was controlled by a temperature controller unit. The flow rate, differential pressure, temperature, and liquid level were monitored by a data acquisition unit connected to a PC. In the experiments, the superficial gas and liquid velocities were varied. Three four-sensor probes or electromagnetic probes were installed at three different axial positions ($z/D = 3.2$, 17.6, and 32.4) of the test section to investigate the axial development of two-phase flow structure. In addition, these probes were traversed at 12 radial points to obtain the radial profiles.

11.4 Results and Discussion

11.4.1 Radial Profiles of Two-Phase Flow Properties

The radial profiles of void fraction, interfacial area concentration, liquid velocity, and turbulence intensity are shown in Fig. 11.4. The horizontal axis is the radial position from the pipe center to the pipe wall, and the vertical axis is the measured data. The void fraction increases along the flow direction, mainly as a result of the static pressure change. The void fraction profile at $z/D = 3.2$ seems to be uniform and shows a flat shape. As increasing z/D, the void fraction profile changes to core peak because the large bubble moves to the core region. The interfacial area

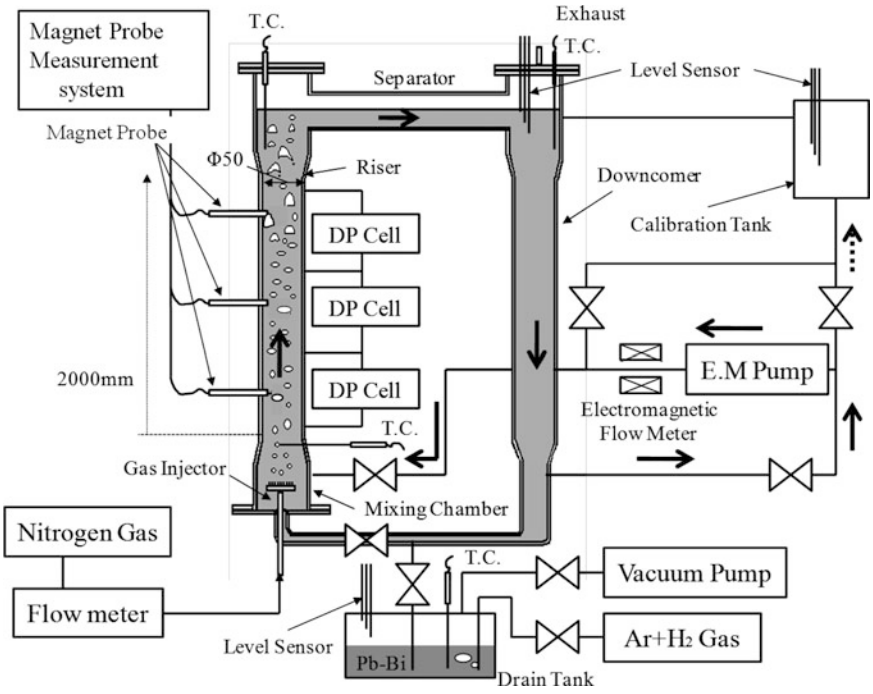

Fig. 11.3 Experimental setup for lead–bismuth-eutectic (LBE) two-phase flow measurement

concentration also increases as increasing z/D, as shown in Fig. 11.4b. The axial liquid velocity profiles are shown in Fig. 11.4c. The dashed lines are the calculated value of seventh power law, as follows:

$$U(r) = U_{\max}\left(1 - \frac{r}{R}\right)^{1/7} \tag{11.1}$$

where $U_{\max}$ is the measured velocity at the pipe center. The measured liquid velocity profile at $z/D = 32.4$ has a core peak, although the profiles at $z/D = 3.2$ and 17.6 have a wall peak. Thus, the liquid velocity profiles were also developed axially and the gas–liquid interfacial drag force caused by the rising bubbles might act on the liquid phase. The turbulence intensity profiles in the liquid metal two-phase flow have a wall peak and they increase with the increase of z/D. These profiles have a shape similar to that in an air–water two-phase flow. However, the nondimensional turbulence intensity was much larger than the measured result in air–water flow systems; this might be attributed to the smaller liquid velocity in the present experimental condition, where the bubble-induced turbulence may be dominant.

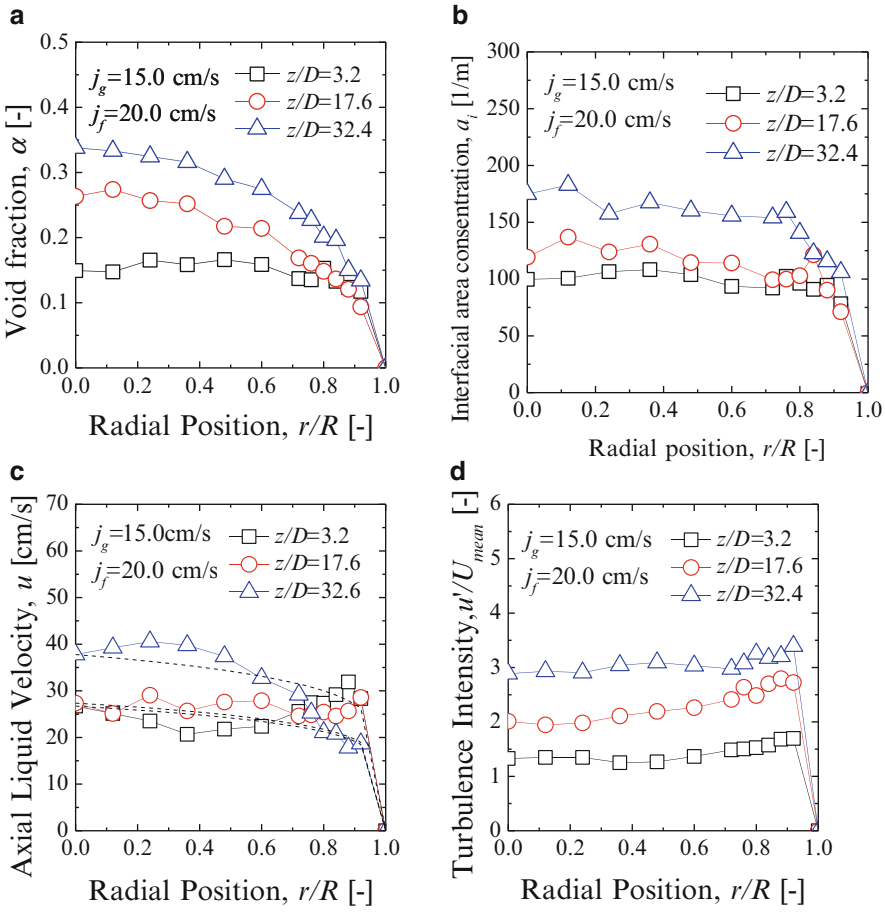

Fig. 11.4 Typical measurement results: void fraction (**a**), interfacial area concentration (**b**), axial liquid velocity (**c**), and turbulence intensity (**d**)

11.4.2 Comparison of Interfacial Area Concentration

Interfacial area concentration measured by the four sensor probes was compared with existing correlations (Fig. 11.5). The vertical axis shows the estimation error between the measured and calculated interfacial area concentration. All the correlation overestimates the interfacial area concentration by 50–90 %, which might be caused by the differences in bubble size and shape. Most of the correlations were formulated with air–water two-phase flow data for a bubbly flow regime. However, the bubble shape in a liquid metal two-phase flow might be strongly distorted by the momentum exchange at the gas–liquid interface. Thus, a more appropriate expression of the interfacial area concentration for liquid metal two-phase flow should be developed based on the experimental database.

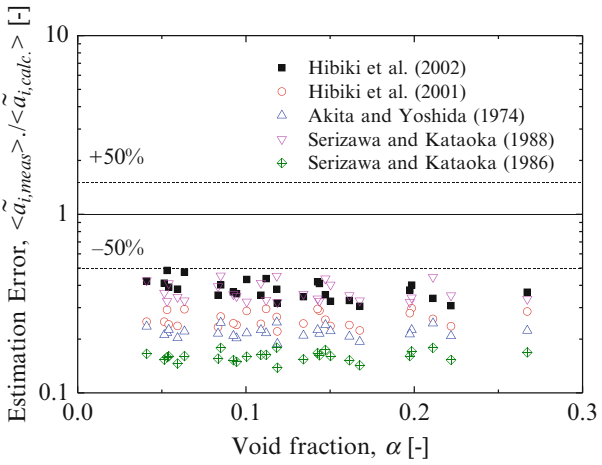

Fig. 11.5 Comparison of interfacial area concentration with existing correlations

11.4.3 Bubble-Induced Turbulence

The turbulence intensity measured in this study could be divided into wall turbulence and bubble-induced turbulence. However, turbulent production from bubbles is dominant at the pipe center. Thus, the turbulence intensity at $r/R = 0$ was plotted against the void fraction measured by the four-sensor probe (Fig. 11.6). In addition, the present results were compared with the previous experimental data of the bubble-induced turbulence in an air–water two-phase flow system. The solid line in this figure denotes the calculated value by the following semi-theoretical equation [5].

$$u' = u_r \alpha^{0.5}. \tag{11.2}$$

In this equation, the velocity field around the bubble is assumed as potential flow and the rotational component of the wake is ignored. In addition, the value calculated by the empirical equation for air–water two-phase flow [6] is also drawn as the dashed line in Fig. 11.6; the equation is represented as follows:

$$u' = 0.85\alpha^{0.8}. \tag{11.3}$$

Although the fluid properties are different with the air–water two-phase flow, the measured turbulence intensity agrees with Eq. (11.3) and the previous data [7–9], except the result at $z/D = 3.2$. However, Eq. (11.3) was derived for an air–water flow system and its applicability to liquid metal flow was not clear. Therefore, the mechanism of turbulence production in liquid metal two-phase flow should be investigated in more detail. On the other hand, the turbulence intensity at $z/D = 3.2$ was slightly larger than other plots and Eq. (11.3). The measurement

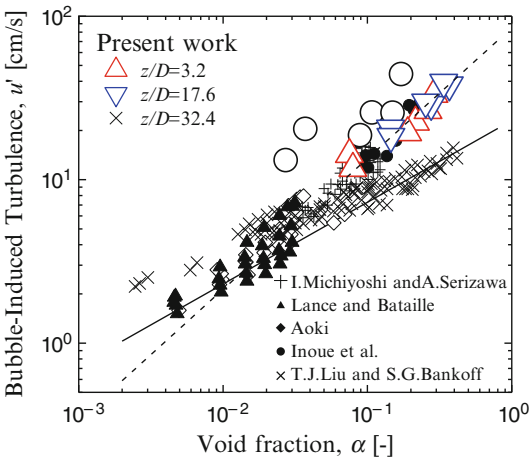

Fig. 11.6 Bubble-induced turbulence

position at $z/D = 3.2$ was relatively close to the gas injector, so it is expected that the flow was not fully developed.

11.5 Conclusions

A liquid metal two-phase flow was investigated by using a four-sensor probe and an electromagnetic probe. From the measurement results of two-phase flow structure and turbulence characteristics, the following knowledge was obtained.

- Radial profile of void fraction changes from wall peak to core peak along the flow direction.
- Axial development of the liquid velocity field shows different tendency for the void fraction profiles.
- Existing correlations for interfacial area concentration overestimate interfacial area concentrations at present experimental conditions, which might be attributed to the difference in bubble size. A new correlation should be modeled with further consideration of bubble size and the wall conditions.
- Bubble-induced turbulence at the pipe center in lead–bismuth two-phase flow agrees well with the previous experimental data for air–water flows. However, the mechanism should be clarified by measuring the liquid–metal two-phase flow in a wide range of flow conditions.

References

1. Tsujimoto K, Sasa T, Nishihara K, Oigawa H, Takano H (2004) Neutronics design for lead–bismuth cooled accelerator-driven system for transmutation of minor actinide. J Nucl Sci Technol 41(1):21–36
2. Saito Y, Mishima K (2012) Bubble measurements in liquid-metal two-phase flow by using a four-sensor probe. Multiphase Sci Technol 24:279–297
3. Ricou R, Vives C (1982) Local velocity and mass transfer measurements in molten metals using an incorporated magnet probe. Int J Heat Mass Transfer 25(10):1579–1588
4. Iguchi M, Tokunaga H, Tatemichi H (1997) Bubble and liquid flow characteristics in a Wood's metal bath stirred by bottom helium gas injection. Metall Mater Trans B 28B:1053–1061
5. Larce M, Bataille J (1983) Turbulence in the liquid phase of a bubbly air-water flow. In: Advances in two-phase flow and heat transfer, fundamentals and applications, vol 1. Martinus Nijhoff Publishers, Boston, pp 403–427
6. Michiyoshi I, Serizawa A (1986) Turbulence in two-phase bubbly flow. Nucl Eng Des 95:253–267
7. Aoki S (1982) Eddy diffusivity of momentum in bubbly flow. M.S. thesis, Department of Nuclear Engineering, Kyoto University
8. Inoue A, Aoki S, Koga T, Yaegashi H (1976) Void-fraction, bubble and liquid velocity profiles of two-phase bubble flow in a vertical pipe. Trans JSME 42:2521–2531
9. Liu JT, Bankoff GS (1993) Structure of air-water bubbly flow in a vertical pipe. I. Liquid mean velocity and turbulence measurements. Int J Heat Mass Transfer 36(4):1049–1060